



Original Research Article

Investigating the Performance of Rural Off-Grid Photovoltaic System with Electric-Mobility Solutions: A Case Study Based on Kenya

Aminu Bugaje ^{*1}, Mathias Ehrenwirth¹, Christoph Trinkl¹, Wilfried Zoerner¹

¹Institute of new Energy Systems, Technische Hochschule Ingolstadt
Esplanade 10, 85049, Ingolstadt, Germany
e-mail: Aminu.Ilyasubugaje@thi.de

Cite as: Bugaje, A., Ehrenwirth, M., Trinkl, C., Zoerner, W., Investigating the Performance of Rural Off-Grid Photovoltaic System with Electric-Mobility Solutions: A Case Study Based on Kenya, *J. sustain. dev. energy water environ. syst.*, 10(1), 1090391, 2022, DOI: <https://doi.org/10.13044/j.sdewes.d9.0391>

ABSTRACT

Over the last years, stand-alone and / or hybrid photovoltaic systems have spread in rural areas, especially in Sub-Saharan Africa. Compared to conventional systems (typically diesel generators), these systems can provide a reliable electricity supply at reasonable costs with a low degree of greenhouse gas emissions. Therefore, this paper focuses on modelling and investigation of an off-grid photovoltaic system (charging station) performance based on a located in Kenya. However, the model can be adapted to any other region and any type of photovoltaic systems module by changing model input data such as solar radiation, air temperature, longitude, latitude, load profile and standard test conditions parameters of the photovoltaic systems module. The modelled photovoltaic system (charging station) will be used to provide reliable and clean electricity for a number of important tasks (e.g. water purification, charging special floatable lanterns and electric bikes).

KEYWORDS

Lake Victoria, Photovoltaic, Off-grid, Charging station, Model, Sub-Saharan Africa, Electric mobility.

INTRODUCTION

In SSA, most of the rural electrification is carried out by governments through the extension of the national grid which is technically challenging and expensive to implement due to the inaccessibility and sparseness of most of Sub-Saharan Africa (SSA's) rural areas [1].

Similarly, apart from the lack of access to electricity in rural communities of SSA, access to safe drinking water is still a luxury in SSA rural communities. In this region, only approximately 60% of people have access to safe drinking water and only half have access to improved water sources [2]. Lack of safe drinking water causes many direct health problems which leads to the death of millions of people especially children [3].

The majority of SSA's rural settlers rely on bicycle taxis, animal-driven carts and old vehicles that mostly run inefficiently at low speed with high fuel consumption and greenhouse gas (GHG) emissions. Most of the young people walk over long distances to schools or tend to use poor transport services, which contributes to late enrolment or early drop-out [4]. Women and children have to walk over a long distance to fetch (untreated) water from the lakes or wells

* Corresponding author

for domestic usages. As a result, this makes them vulnerable to diseases, poverty and gender inequality [5].

Over the years, standalone diesel generators were the most common off-grid electrical power source in rural locations [6]. However, high fuel and maintenance costs are problematic for owners. A study by [7, 8] shows that the cost of diesel in Rwanda relative to other countries in Africa is high due to fuel taxation. Logistical barriers in Brazil also increase the costs of diesel by 15% - 45% [9].

In recent times, due to decreasing cost of photovoltaic (PV) technology and abundant solar irradiation in SSA regions, solar off-grid PV systems are gaining momentum in SSA's rural electrification projects because off-grid PV systems are one of the viable solutions to the modern energy supply in the SSA region. These projects cover PV installations in various institutions such as rural health care centres, schools, street lighting, communication, and water pumping etc [10].

An off-grid PV system comprises a solar array, a maximum power point tracker/charge controller, an inverter, battery bank and electrical energy. Typically, hybrid systems are used together with a diesel generator to provide backup power when there is insufficient power generated from the PV array or batteries [8].

The performance of PV based systems can be significantly affected by their orientation and any type of solar tracking capability. A study reported that the optimum orientation for a fixed array slope should be as local latitude plus 10° [11], while the results of other studies indicate that the best slope for a fixed array should simply be equal to the local latitude [12]. Authors in [13] cite that angles of the local latitude plus 8° – 15° are the best array tilt angles. In addition, optimum tilt varies at fixed latitude, probably due to seasonal weather variations such as clouds or fog throughout the year [14].

Subsequently, the performance of a PV array also depends on the operating conditions, i.e., depends not only on solar irradiation and temperature but also on the array configuration and shading effects. The shading effects, for instance, due to a passing cloud or neighbouring buildings cause not only power losses, but also further non-linear effects on the I - V characteristics [15]. Power electronic converters have been developed for integrating renewable energy sources with the other alternating current (AC) electric systems [16].

Proper design of solar PV systems is important to avoid oversizing or under-sizing the system, resulting in either excessive capital costs or insufficient solar electricity production [10]. However, to acquire optimum PV module output, maximum power point tracking (MPPT) systems are therefore very important in solar PV systems design and implementation [10].

Therefore, this paper presents the results of a modelled PV system (charging station) that will later be implemented around Lake Victoria in order to provide reliable and clean electricity for water purification as well as for charging special floatable lanterns for night fishing, charging batteries for electric bikes for water and local transportation.

METHODS

This research makes use of scenarios to describe the design of an off-grid PV charging station for electric mobilities in terms of energy demands around Lake Victoria in Kenya. By combining real-life measurements of different driving conditions and modelling tools, qualitative and quantitative results are generated.

In this paper, the Conventional and Renewable Energy Optimization Toolbox (CARNOT) is used as a tool for modelling an appropriate PV system size to cover the demand requirements. Similarly, Matrix Laboratory (MATLAB) is also used as a tool for generating a realistic demand scenario considering moon phase seasonal fluctuations using the lunar calendar. During low moonlight intensity, less fishing demand is recorded, while high fishing demand is recorded during high moonlight intensity.

Modelling of a yield simulation requires a time-series of input data like solar irradiation, ambient temperature, energy profile and other technical parameters of the planned PV systems [17].

CARNOT tool allows a MATLAB / Simulink time-series assessment of the system's energy production, consumption, battery state of charge (SOC), inverter efficiency, energy deficit. The PV output ($P_{PV,t}$) is obtained using the conversion efficiency of the panels η_{PV} at a given temperature (T_t) and irradiance (G_t), the panel area (A), and the number of panels n as [8]:

$$P_{PV,t} = \eta_{PV} \times G_t \times n \times A \quad (1)$$

The efficiency of the array, which is related to the temperature T_t and irradiance G_t is calculated using:

$$\eta_{PV} = \eta_{nom} + CG(1000 - G_t) + (T_t - 25) \quad (2)$$

$\eta_{PV} = \eta_{nom} + CG(1000 - G_t) + (T_t - 25)$ The CARNOT tool uses a block set called 'PV module' to simulate and calculate the output power (P) of the PV module in W based on the module characteristic parameters such as [18]:

$$P = \frac{S_R}{I_R} IAM \times P_{max} \left[1 - \left(T_a + T_d \frac{S_P}{I_R} \right) - M_T \right] \quad (3)$$

where: P - output power of the PV module in W; S_R - solar radiation; I_R - incident radiation at STC: 1000 W/m²; IAM - incidence angle modifier: 1 for vertical direct solar radiation. It follows the reflection law of Fresnel; P_{max} - peak power (W_p) at STC in W; T_a - ambient temperature; T_d - temperature difference to ambient at full solar radiation (1000 W/m²): 40 K; S_P - solar power; M_T - module temperature at STC: 25 °C.

Figure 1 shows the PV charging station model using CARNOT block set in a MATLAB / Simulink environment. The model consists of weather data, PV modules, inverters, batteries and electric energy profile.

The block set named 'weather_data' in **Figure 1a** serves as input to the system and holds the weather data of Mbita town along Lake Victoria in Kenya. The weather data was obtained from the Meteorom weather database. The weather data contained information such as temperature, solar irradiation, humidity, precipitation, wind speed etc.

The block set named 'PV_orientation' in **Figure 1a** serves as input to the system and holds the PV module orientation in terms of tilt and azimuth angle. In this study, a tilt angle of 12° and azimuth angle of 180° was chosen for better PV system performance as mentioned by [13].

The block set named 'Inv_capacity' in **Figure 1a** holds the inverter nominal power in kVA and the block set 'Inverter' simulates and calculates the photovoltaic alternating current (PV_AC) power considering the efficiency of the inverter based on a lookup table for different part-energy and over-energy conditions.

The block set named 'battery' in **Figure 1b** calculates the maximum amount of power that the storage bank can absorb. The block set named 'Energy demand' serves as input to the system and holds the generated electric energy demands in kWh for water purification, fishing lamps, and portable batteries for e-bikes. The battery module uses PV_AC and energy demand as inputs, where it takes the difference between the PV_AC and energy demand. Whenever PV_AC is higher than energy demand, the battery absorbs all available surplus PV_AC power for charging purposes. Whenever PV_AC is lower than energy demand, the battery discharges to serve the energy demand due to low PV_AC produced. The maximum charge power varies

from one-time step to the next according to its state of charge and its recent charge and discharge history.

Subsequently, for system (charging station) performance analysis, solar irradiation, battery state of charge (SOC), PV production, energy deficit (Punder) and battery discharge were considered as the output of the system as shown in **Figure 1a** and **Figure 1b**.

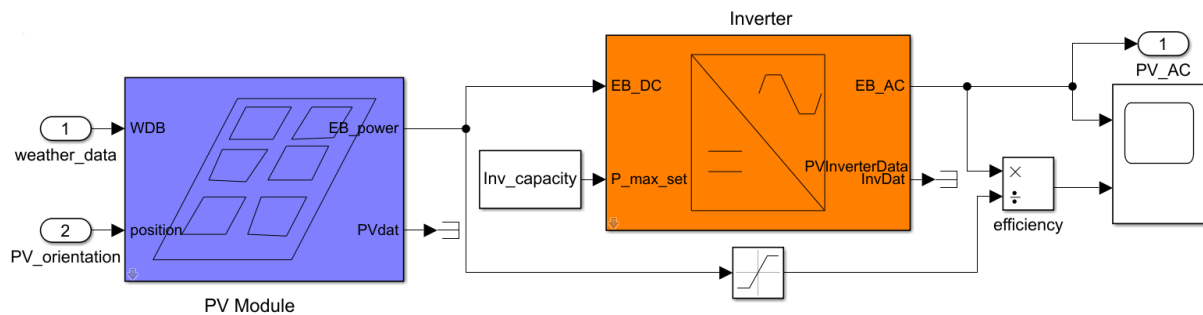


Figure 1a MATLAB / Simulink CARNOT model of the PV system

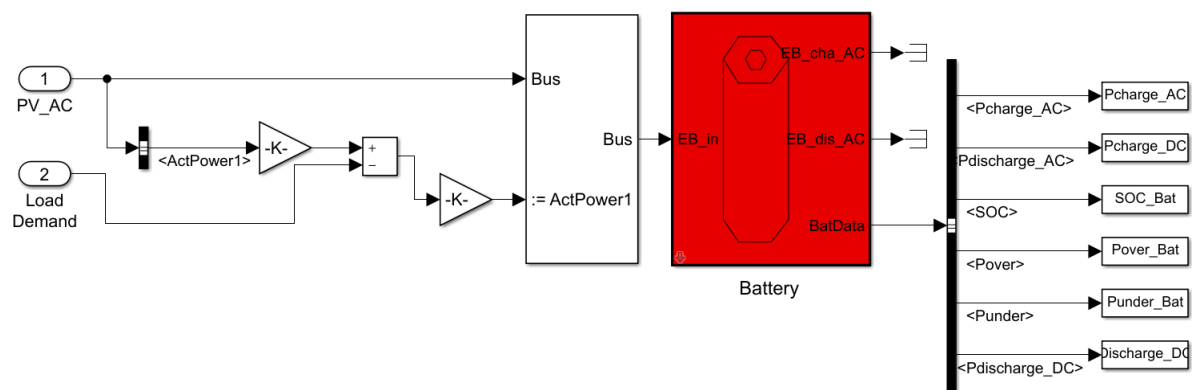


Figure 1b. MATLAB / Simulink CARNOT model of the PV system

SELECTION OF CASE STUDY AREA

Mbita is situated on the shorelines of Lake Victoria in Homa Bay County, one of 47 counties in Kenya (**Figure 2**). It is a remote area that lies on latitudes $0^{\circ} 21'$ and $0^{\circ} 32'$ south and longitudes $34^{\circ} 04'$ and $34^{\circ} 24'$ east. It lies approximately 400 km west of Nairobi, the capital of Kenya, and covers a total area of 163.28 km². Mbita is home to the International Centre for Insect Physiology and Ecology (ICIPE) research compound, Tom Mboya Mausoleum, Remba Island, Mfangano Island, Rusinga Island and several tourist attractions [19].

Moreover, trading appeared to be one of the key sources of income for the people of Mbita Town. Similarly, fishing is also an important economic activity in Homa Bay County, with the county controlling over 80% of the Lake Victoria Beach front in Kenya. Mbita Town is a leading fishing region with over 80% of its residents being fishermen [19].

Consequently, the coastline of Lake Victoria is becoming increasingly populated. People from other parts of the country are coming to the lake, hoping for a secure livelihood. Therefore, the ecosystem of Lake Victoria is severely endangered as daily untreated industrial wastewater, pesticides, boat fuel and trash end up in the lake [20].

Moreover, the proximity of Lake Victoria to Kenya's largest city, Kisumu, does not ensure access to clean water, particularly in the rural communities of Kisumu [21]. Similarly, the people and fishermen living around Mbita Town and Lake Victoria depend heavily on gasoline-powered boats and motorcycles respectively, for the transport of people and goods

and this presents clear disadvantages in terms of negative externalities such as pervasive noise, increased local air pollution and greenhouse gas emissions [22].

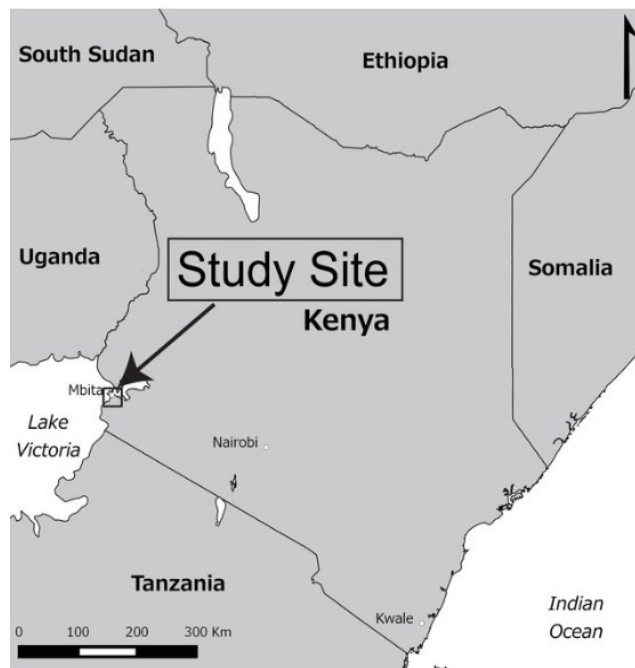


Figure 2. Study Location: Mbita, Kenya along the shore of Lake Victoria [23]

DESIGN SCENARIO DESCRIPTION

In this research, scenarios are applied to describe the potential development of the off-grid PV system (charging station) energy supply and electricity load demand in the selected location. The scenarios have been categorised into two by considering the average daily distance covered by the electric bikes and the energy consumption of the electric bike in kWh/100 km (Table 1). It can be seen in Table 1 that design scenario 1 considers 50 km as daily distance e-bikes while design scenario 2 considers 100 km as daily distance covered by e-bikes.

Table 1. Different System Design Scenarios

System Design Scenario	E-bikes Daily Target	E-bikes Daily Distance Covered in km	E-bikes Daily Battery Required	E-Lanterns Daily Target	Average Daily Energy Demand in kWh	Annual Energy Demand in kWh
Design 1	40	50	45	400	153	55,846
Design 2	40	100	90	400	275	100,485

In design scenario 1, a PV capacity of 50 kWp and 50 kVA inverter were considered for the modelling. A battery capacity of 208 kWh with a usable capacity of 120 kWh (60% depth of discharge (DOD)) was also considered for the modelling. The SOC represents the available energy in the battery as a percentage. The maximum and minimum SOC of the battery bank is assumed to be 100% and 40% respectively in order to avoid overcharging and undercharging of battery.

In design scenario 2, a PV capacity of 80 kW_P and 80 kVA inverter were considered for the modelling. A battery capacity of 306 kWh with a usable capacity of 183 kWh (60% depth of discharge (DOD)) was also considered for the modelling. The SOC represents the available energy in the battery as a percentage.

MODEL INPUT DATA

For successful modelling of the PV system (charging station), the following must be considered as input to the model.

Weather data of the selected location

In order to model and simulate the PV system (charging station) for the selected location, weather data is necessary in order to serve as input to the model. The weather data was obtained from the Meteonorm weather database. The weather data contained information such as temperature, solar irradiation, humidity, precipitation, wind speed etc. **Figure 3** shows the global solar irradiation and temperature of the selected location. The selected location has an average annual temperature and annual global irradiation of 25.13 °C and 2095 kW/m² respectively. It can be seen from **Figure 3** that the months of March, April and May have the highest solar irradiation while July, December, January and February have the lowest solar irradiation.

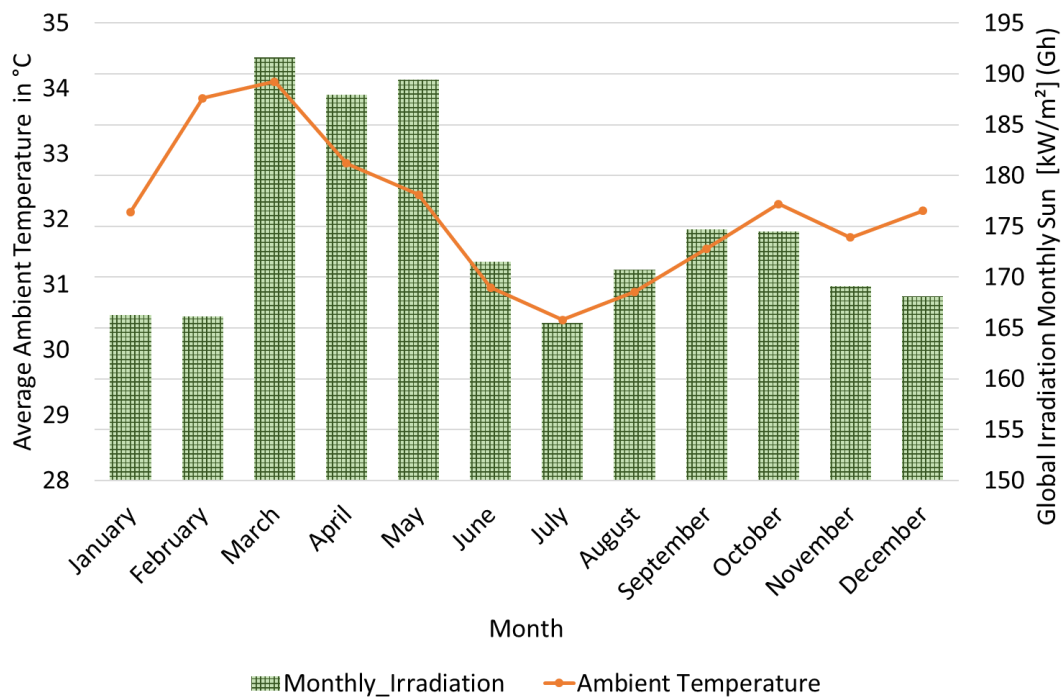


Figure 3. Solar irradiation and ambient temperature of the selected location

Energy estimation

The load profiles of the major load (see **Figure 4**) for electric bikes, fishing lanterns and auxiliary devices (charging station internal consumption) required at Mbita charging station considering measurement data collected are shown in **Table 2a – Table 2e**. Realistic runtimes for the energy demand of the aforementioned major loads had been estimated and the annual energy profiles were generated for workdays and holidays based on seasonal fluctuations (e.g. fishing quotas around moon phase). In case of workdays, fishing lamps, auxiliary devices (i.e. water purification, pumping machine, light bulbs etc.) and mobile batteries for e-bikes are

charged daily due to no moon or low moon light intensity while in holidays, every load is charged except that a smaller number of fishing lamps are charged due to full moon or high moonlight intensity. **Table 2a – Table 2e** shows a detailed information of the major electric demands considering 100 km as default daily distance covered by the e-bikes.

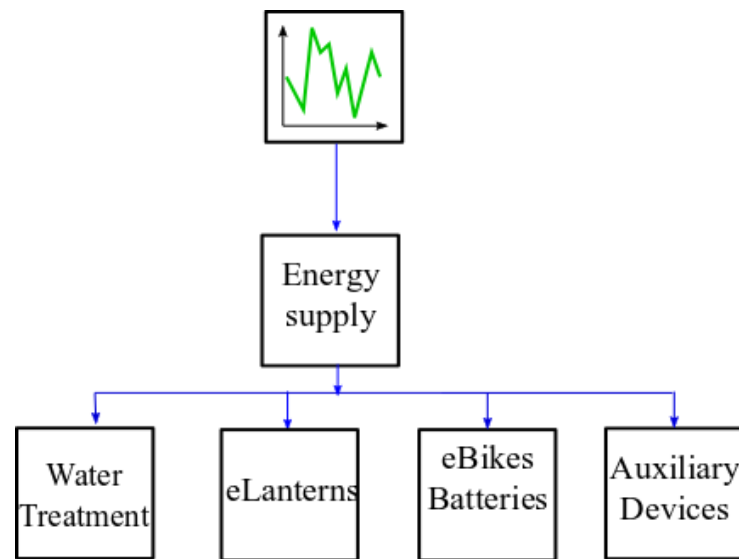


Figure 4. Energy demands

Table 2a. Load profile of E-cargo Bikes @ 100 km daily travelled distance generated for Mbita charging station

Energy Required (Wh)	2200
Charging Rate (W)	200
Charging Time (h)	11
Daily Quantity of bikes	10
Energy Consumption (kWh/100 km)	4.23
Passenger + Load Average Mass (kg)	102
Quantity of Batteries per 100 km	22
Estimated Total Daily Energy (kWh)	48

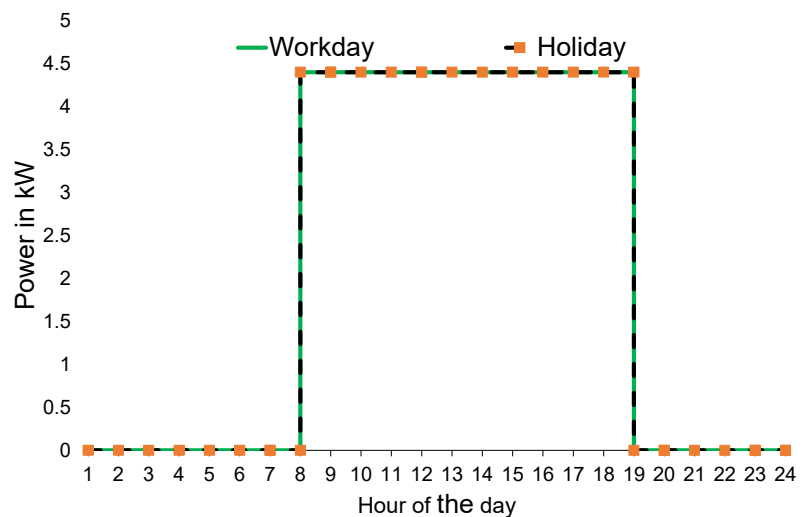


Table 2b. Load profile of E-Opi Bikes @ 100 km daily travelled distance generated for Mbita charging station

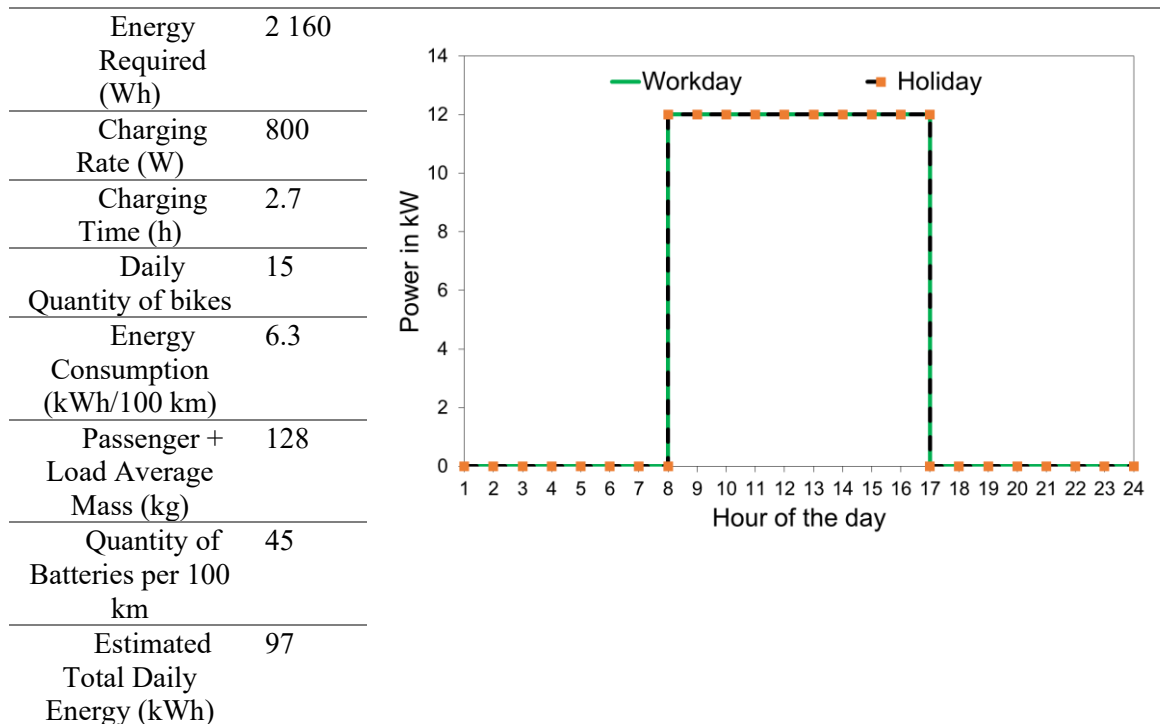


Table 2c. Load profile of E-BodaWerk Bikes @ 100 km daily travelled distance generated for Mbita charging station

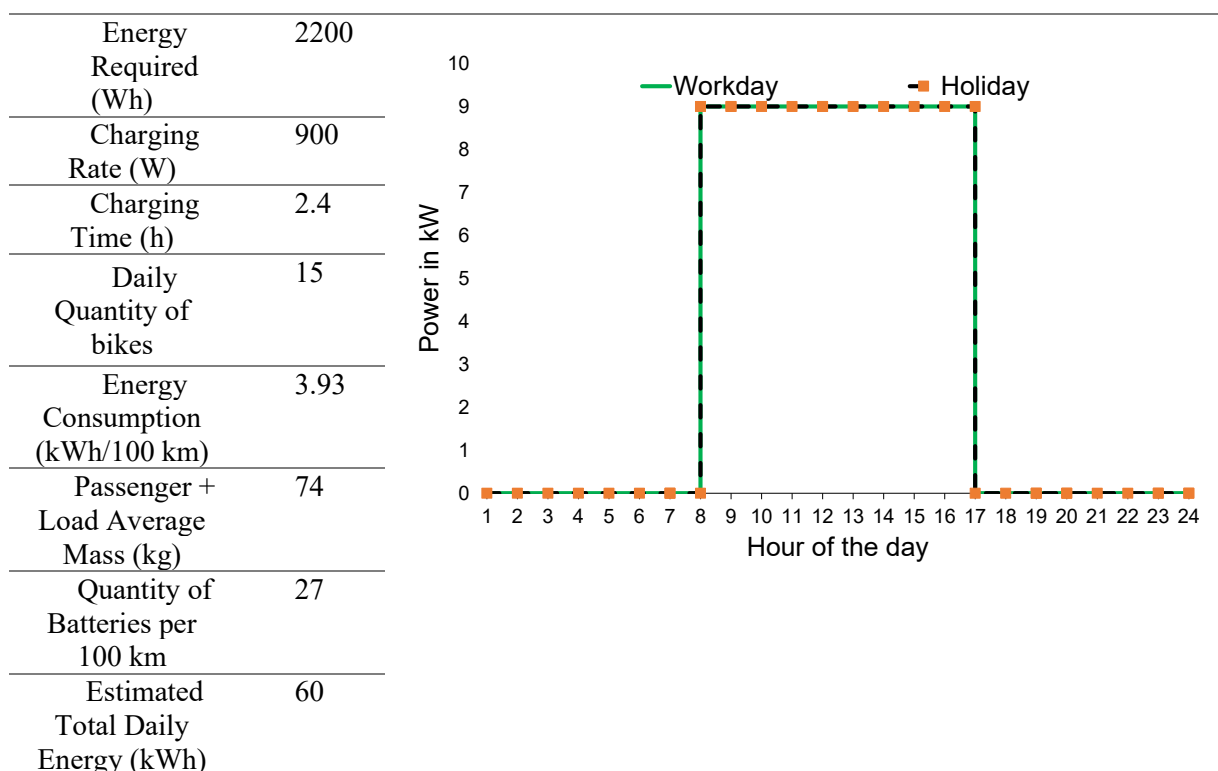


Table 2d. Load profile of E-Fishing Lanterns generated for Mbita charging station

Energy Required (Wh)	110
Charging Rate (W)	37
Charging Time (h)	2.9
Daily Quantity of Lanterns	400
Estimated Total Daily Energy (kWh)	44

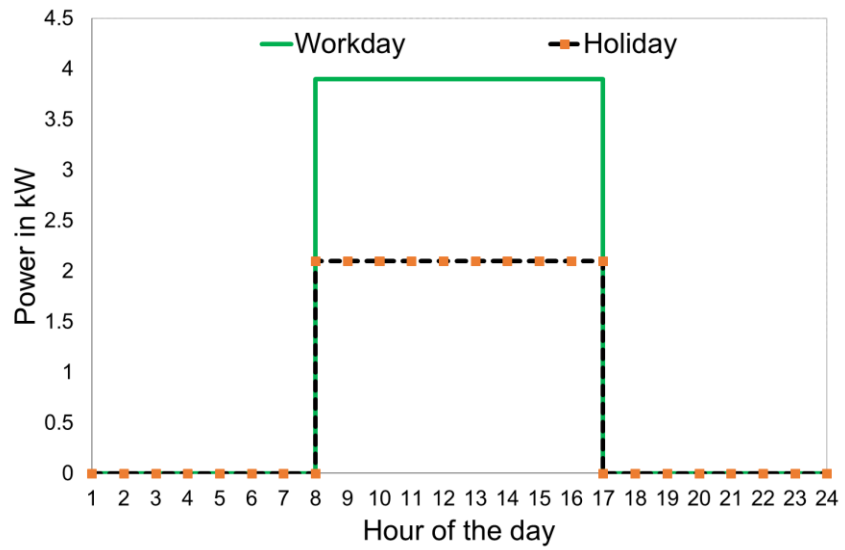
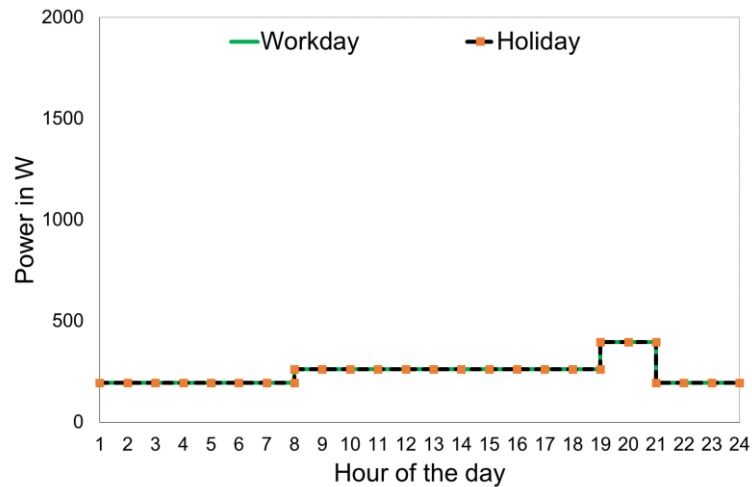


Table 2e. Load profile of Charging Station Auxiliary Devices required at Mbita charging station

Energy Required (Wh)	10 -300
Charging Rate (W)	10 - 80
Charging Time (h)	24
Estimated Total Daily Energy (kWh)	5.7



A daily energy demand profile of 281 kWh and 264 kWh are generated for workdays and holidays considering 100 km as daily distance covered by e-bikes. The hourly accumulated daily electrical demand profile during workdays (days with no full moon) and holidays (days with full moon) with specification peak power of 29.6 kW and 27.8 kW respectively are shown in **Figure 5**. Annual energy demand of 100,485 kWh has been generated (see **Figure 6**).



Figure 5. Accumulated daily electrical demand profile during workdays and holidays considering 100 km as daily distance covered by e-bikes

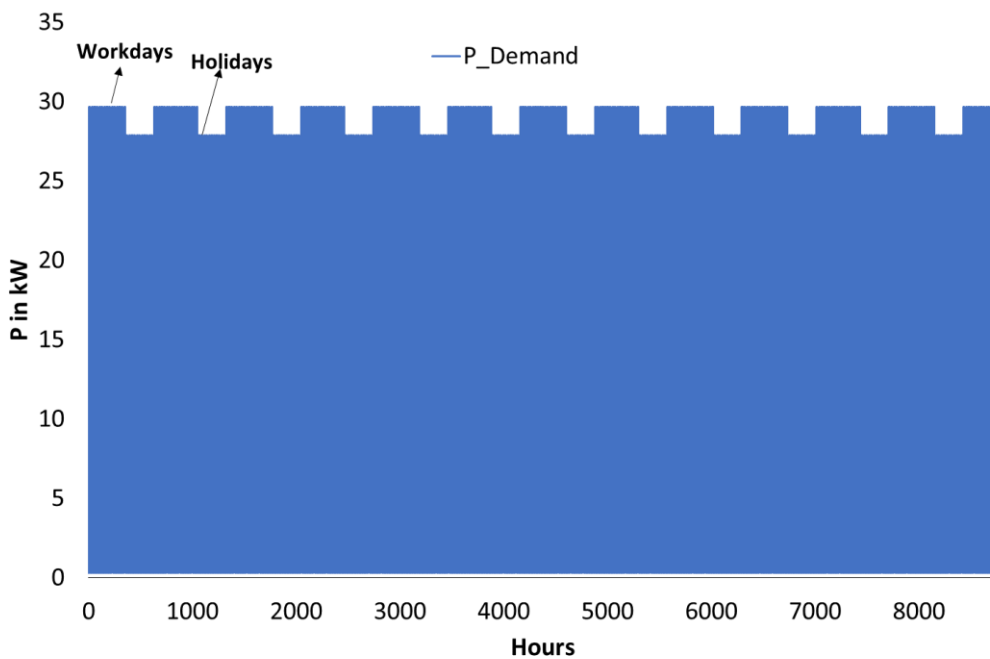


Figure 6. Annual hourly electrical demand profile during workdays and holidays considering 100 km as daily distance covered by e-bikes

MODEL RESULTS AND DISCUSSION FOR DESIGN SCENARIO 1

Figure 7 shows the monthly annual energy demand including seasonal fluctuation (fishing based on moon phase) and it can be seen that month of January and other months with 31 days have the highest energy demand while February being the month with 28 days has the lowest energy demand. Figure 7 also shows the monthly annual PV energy production and it can be

seen that month of May has the highest PV energy production while January and December have the lowest PV energy production due to weather conditions.

Figure 7 also shows the monthly energy deficit, and it can be that April, May and June have the lowest energy deficit. January has the highest energy deficit of 230 kWh, followed by December with 102 kWh energy deficit due to weather conditions. Figure 8 shows the annual hourly PV power production, annual hourly electric demand and annual hourly deficit in kW. An annual PV production of 72,726 kWh, annual energy demand of 55,845 kWh and annual energy deficit of 351 kWh were respectively obtained.

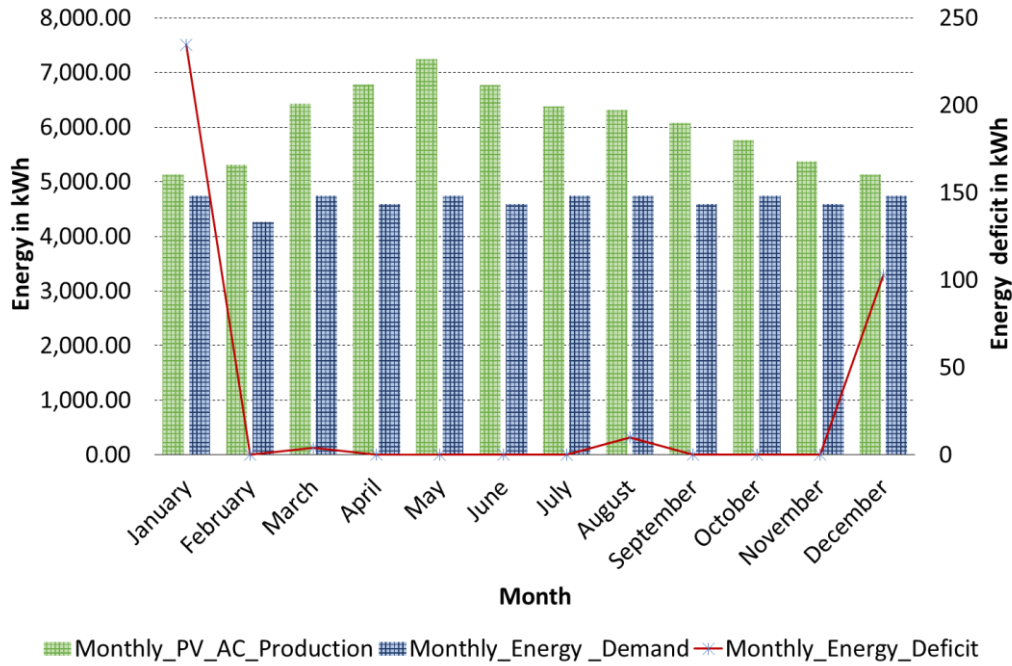


Figure 7. Monthly PV energy production, electric load energy demand and electric load energy deficit in kWh

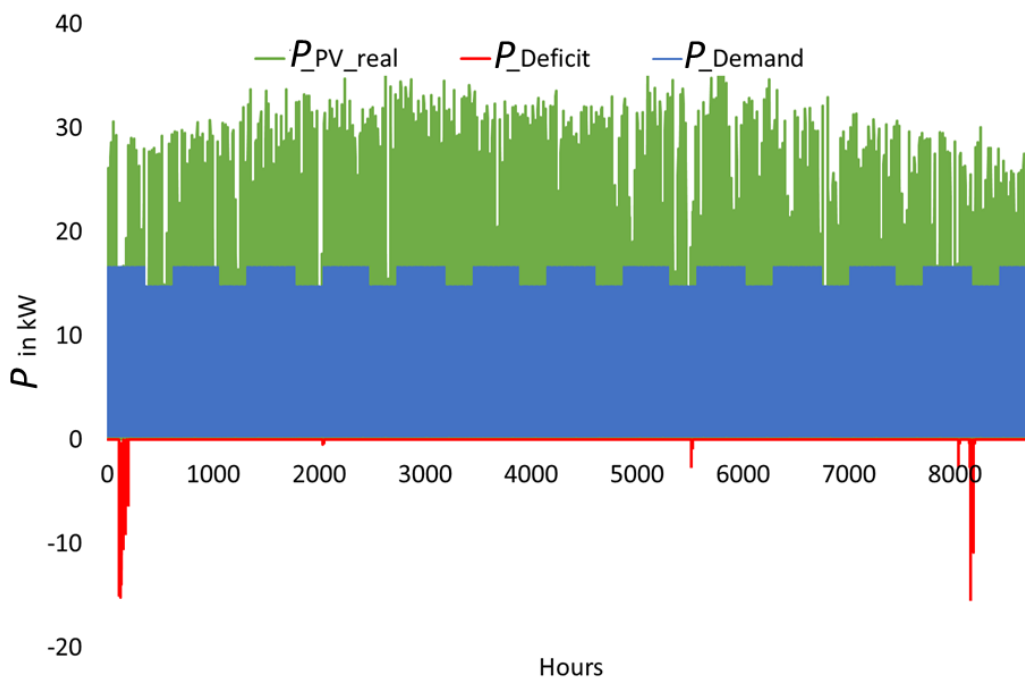


Figure 8. Annual hourly PV power production, demand and deficit in kW

MODEL RESULTS AND DISCUSSION FOR DESIGN SCENARIO 2

Figure 9 shows the monthly annual energy demand including seasonal fluctuation (fishing based on moon phase) and it can be seen that month of January and other months with 31 days have the highest energy demand while February been the month with 28 days has the lowest energy demand.

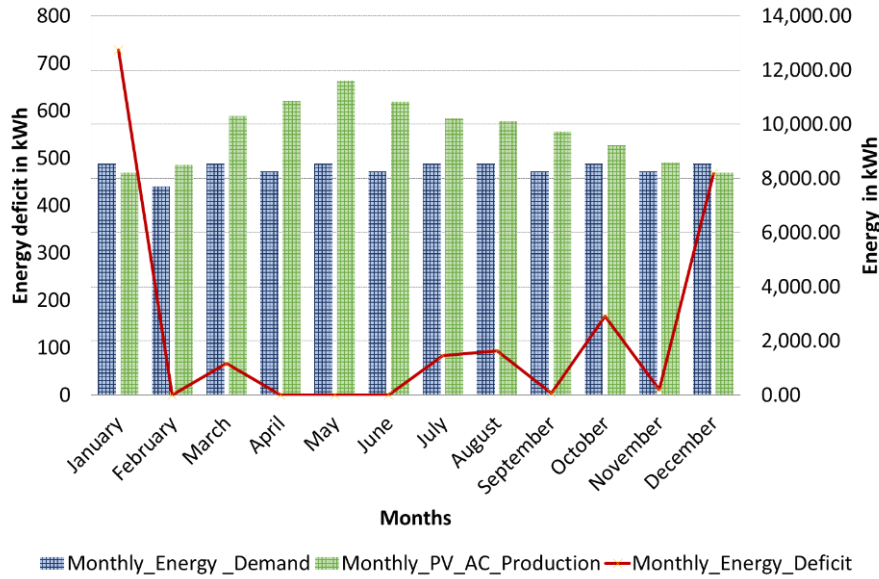


Figure 9. Monthly PV energy production, electric load energy demand and electric load energy deficit in kWh

Figure 9 also shows the monthly annual PV energy production and it can be seen that month of May has the highest PV energy production while January and December have the lowest PV energy production due to weather conditions.

Figure 9 also shows the monthly energy deficit, and it can be that April, May and June have the lowest energy deficit. January has the highest energy deficit of 728 kWh, followed by December with 467 kWh due to weather conditions. Figure 10 shows the annual hourly PV power production, annual hourly electric demand and annual hourly deficit in kW. An annual PV production of 120,450 kWh, annual energy demand of 100,485 kWh and annual energy deficit of 1,623 kWh were respectively obtained.

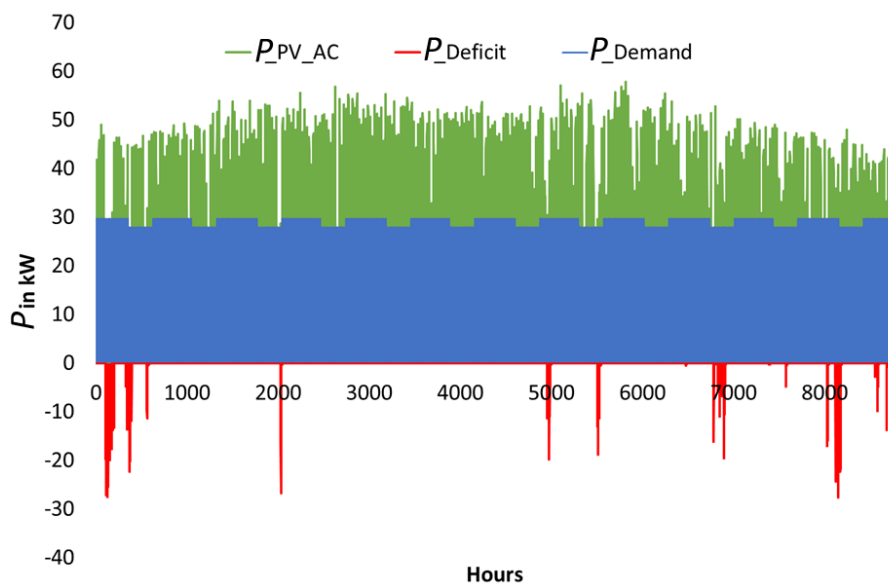


Figure 10. Annual hourly PV power production, demand and deficit in kW

CONCLUSION

This paper investigated the performance of a rural off-grid PV system (charging station) with electric-mobility solutions (i.e. mobile batteries for e-bikes) using MATLAB / Simulink / CARNOT 7.0 Toolbox. Analysis of the PV production, energy consumption and energy deficit were carried out. PV system size and performance strongly depend on metrological variables such as solar irradiation, wind speed and ambient temperature. Consequently, the results obtained show an annual energy deficit of approximately 351 kWh and 1623 kWh for system design scenarios 1 and 2 respectively which means, the system could not cover the whole energy demand due to the aforementioned variabilities of a PV system.

Therefore, in order to avoid using diesel generator or grid connection for energy deficit reduction. A load management algorithm will be presented in future works to optimally integrate the electric mobility solutions into the rural off-grid PV system charging station. The load management algorithm will capture the maximum amount of variable solar generation, which then sizes and schedules a finite number of devices to track available solar PV power.

ACKNOWLEDGEMENT

The authors would like to thank Siemens Stiftung for funding this work under the eMobility Kenya (WeMobility solutions) project.

NOMENCLATURE

A	panel area	$[m^2]$
CG	irradiance coefficient	$[W/m^2]$
G_t	irradiance	$[W/m^2]$
G_h	global horizontal irradiance	$[W/m^2]$
IAM	incidence angle modifier	$[-]$
I_R	incident radiation at STC 1000 W/m ²	$[W/m^2]$
M_T	module temperature at STC	$[^{\circ}C]$
n	number of panels	$[-]$
P	output power of the PV module	$[W]$
$P_{deficit}$	power deficit	$[W]$
P_{demand}	power /electric demand	$[W]$
P_{max}	peak power at STC	$[W]$
P_{PV_real}	PV power produced	$[W]$
S_P	solar power	$[W]$
S_R	solar radiation	$[W/m^2]$
T_a	ambient temperature	$[^{\circ}C]$
T_d	temperature difference to ambient at full solar radiation	$[^{\circ}C]$
T_t	ambient temperature	$[^{\circ}C]$
Greek letters		
η_{PV}	efficiency of solar panel	$[-]$
Abbreviations		
DOD	Battery Depth Of Discharge	
GHG	Greenhouse Gas	
PV	Photovoltaic	
SOC	Battery State Of Charge	
STC	Standard Test Conditions	

REFERENCES

1. C. S. Kaunda, C. Z. Kimambo, and T. K. Nielsen, "Potential of Small-Scale Hydropower for Electricity Generation in Sub-Saharan Africa," *ISRN Renewable Energy*, vol. 2012, no. 2, pp. 1–15, 2012, doi: <http://dx.doi.org/10.5402/2012/132606>.
2. WWP, World Water Assessment. The United Nations World Water Development Report 4, Managing Water under Uncertainty and Risk. WWP (World Water Assessment Programme). United Nations Educational, Scientific and Cultural Organization (UNESCO). [Online]. Available: <https://unesdoc.unesco.org/ark:/48223/pf0000215644> [Accessed: 21-Oct-2019].
3. A. Prüss-Üstün, R. Bos, F. Gore, and Bartram Jamie, "Safer Water, Better Health: Costs, Benefits and Sustainability of Interventions to Protect and Promote Health.," 2008. [Online]. Available: https://apps.who.int/iris/bitstream/handle/10665/43840/9789241596435_eng.pdf?sequence=1 [Accessed: 14-Feb-2021]
4. S. Bloemen, Mobility for Africa. [Online]. Available: <https://www.mobilityforafrica.com/new-blog/> [Accessed: 08-Feb-2019].
5. G. Porter, "Transport Services and Their Impact on Poverty and Growth in Rural Sub-Saharan Africa: A Review of Recent Research and Future Research Needs," *Transport Reviews*, vol. 34, no. 1, pp. 25–45, 2014, doi: <http://dx.doi.org/10.1080/01441647.2013.865148>.
6. P. Díaz, C. Arias, R. Peña, and D. Sandoval, "FAR from the grid: A rural electrification field study," no. 35, 2010, doi: <https://doi.org/10.1016/j.renene.2010.05.005>.
7. S. Szabó, Bódis K, T. Huld, and M. Moner-Girona, "Energy solutions in rural Africa: mapping electrification costs of distributed solar and diesel generation versus grid extension," vol. 6, no. 3, 2011, doi: <https://doi.org/10.1088/1748-9326/6/3/034002>.
8. Crossland, Andrew, F., Anuta, Oghenetjiri, H., and Wade, Neal, S., "A socio-technical approach to increasing the battery lifetime of off-grid photovoltaic systems applied to a case study in Rwanda," vol. 83, pp. 30–40, 2015, doi: <http://dx.doi.org/10.1016/j.renene.2015.04.020>.
9. A. Schmid and C. A. Hoffmann, "Replacing diesel by solar in the Amazon: short-term economic feasibility of PV-diesel hybrid systems," vol. 32, no. 7, pp. 881–898, 2004, doi: [https://doi.org/10.1016/S0301-4215\(03\)00014-4](https://doi.org/10.1016/S0301-4215(03)00014-4).
10. C. Patrick, "Design of rural photovoltaic water pumping systems and the potential of manual array tracking for a West-African village," no. 103, pp. 288–302, 2014, doi: <http://dx.doi.org/10.1016/j.solener.2014.02.024>.
11. M. Hankins, *Solar Electric Systems for Africa, A Guide for Planning and Installing Solar Electric Systems in Rural Africa*. London: Commonwealth Science Council, 1995.
12. M. A. Yakup, M. H.M., and Q. A., "Optimum tilt angle and orientation for solar collector in Brunei Darussalam," vol. 24, pp. 223–234, 2001, doi: [https://doi.org/10.1016/S0960-1481\(00\)00168-3](https://doi.org/10.1016/S0960-1481(00)00168-3).
13. M. Kacira, M. Simsek, Y. Babur, and S. Demirkol, "Determining optimum tilt angles and orientations of photovoltaic panels in Sanliurfa, Turkey," vol. 29, pp. 1265–1275, 2004, doi: <https://doi.org/10.1016/j.renene.2003.12.014>.
14. M. Lave and Kleissl, "Optimum fixed orientations and benefits of tracking for capturing solar radiation in the continental United States," vol. 36, no. 3, pp. 1145–1152, 2011, doi: <http://dx.doi.org/10.1016/j.renene.2010.07.032>.
15. L. Fialho, R. Meli'cio, V. Mendes, J. Figueiredo, and Collares-Pereira, "Amorphous solar modules simulation and experimental results: effect of shading. In: Camarinha-Matos, L.M., Barrento, N.S., Mendonca, R. (Eds.) *Technological Innovation for Collective Awareness Systems*," pp. 315–323, 2014a, doi: https://doi.org/10.1007/978-3-642-54734-8_35.

16. L. Fialho, R. Melício, and V. Mendes, “PV system modeling by five parameters and in situ test. In: Proc. 22th International Symposium on Power Electronics, Electrical Drives, Automation and Motion – Speedam,” pp. 1–6, 2014b, doi: <https://doi.org/10.1109/SPEEDAM.2014.6872097>.
17. A. K. Shukla, K. Sudhakar, and P. Baredar, “Design, simulation and economic analysis of standalone roof top solar PV system in India,” vol. 136, pp. 437–449, 2016, doi: <http://dx.doi.org/10.1016/j.solener.2016.07.009>.
18. Arnold Wohlfeil, CARNOT Toolbox. [Online]. Available: <https://nl.mathworks.com/matlabcentral/fileexchange/68890-carnot-toolbox> [Accessed: 8-Feb-2020].
19. R. Ochieng, URBAN SUSTAINABILITY REVIEW (USR) MBITA: HOMA BAY COUNTY. [Online]. Available: <http://symbiocitykenya.org/wp-content/uploads/2017/12/USR-HomabayMbita-highres-Symbiocity.pdf> [Accessed: 22-Nov-2019].
20. KWDT, Katosi Women Development Trust: Uganda: Villages at Lake Victoria obtain drinking water and toilets. [Online]. Available: <https://arche-nova.org/en/project/villages-lake-victoria-obtain-drinking-water-and-toilets> [Accessed: 21-Oct-2019].
21. AFD, Agence française de développement: Kenya: In Kisumu, Lake Victoria’s Water is Becoming Safe to Drink. [Online]. Available: <https://www.afd.fr/en/kenya-kisumu-lake-victorias-water-becoming-safe-drink> [Accessed: 21-Nov-2019].
22. A. Kumar, Understanding the Emerging Role of Motorcycles in African Cities : A Political Economy Perspective. Sub-Saharan Africa Transport Policy Program (SSATP) discussion paper. [Online]. Available: <https://openknowledge.worldbank.org/handle/10986/17804> [Accessed: 27-Nov-2019].
23. T. HOSHI et al., “Spatial Distributions of HIV Infection in an Endemic Area of Western Kenya: Guiding Information for Localized HIV Control and Prevention,” vol. 11, no. 2, 2016, doi: <https://doi.org/10.1371/journal.pone.0148636>.



Paper submitted: 20.10.2020
Paper revised: 14.02.2021
Paper accepted: 16.02.2021